Studies on the Dynamics of Phosphorylated
p-tert-Butylcalix[6]arenes by Using 2D NMR Spectroscopy

Rob G. Janssen,[†] John P. M. van Duynhoven,[‡] Willem Verboom,[†]
Gerrit J. van Hummel,[§] Sybolt Harkema,[§] and David N. Reinhoudt*,[†]

Contribution from the Laboratories of Organic Chemistry, Chemical Analysis, and Chemical Physics, University of Twente, P.O. Box 217, 7500 AE Enschede, The Netherlands

Abstract: The overall dynamics of partially phosphorylated and thiophosphorylated *p-tert*-butylcalix[6]arenes has been studied by NMR spectroscopy. When *p-tert*-butylcalix[6]arene is monosubstituted with a phosphate or thiophosphate group, the calix[6]arene skeleton is remarkably rigidified. The 1,3- and 1,4-(thio)phosphorylated *p-tert*-butylcalix[6]arenes are more flexible. 2D NMR spectroscopy showed that these calix[6]arenes adopt *syn* conformations. A combination of ^{1}H and ^{31}P NMR spectroscopy revealed that the calix[6]arene (thio)phosphates are involved in at least three dynamic processes, *viz.*, macrocyclic ring interconversion, hydrogen bond array reversal, and pinched conformer interconversion. The activation barrier ($\Delta G_m^{\ddagger}$) for macrocyclic ring interconversion depends on the type and number of substituents and ranges from 67 to 86 kJ·mol^{-1}. The activation barrier ($\Delta G_h^{\ddagger}$) for hydrogen bond array reversal depends on the number of hydroxyl groups and ranges from 31 to 45 kJ·mol^{-1}. For the pinched conformer interconversion an activation barrier ($\Delta G_p^{\ddagger}$) ranging from 44 to 55 kJ·mol^{-1} was found. Pinched conformations have been frequently observed in the solid state, for example, for mono- and 1,4-bis(thiophosphorylated) *p-tert*-butylcalix[6]arene. These studies, however, show for the first time that these conformations also exist in solution and that differently pinched conformers may rapidly interconvert.

Introduction

The modular approach in supramolecular chemistry for the synthesis of molecular receptors is now an established methodology. We have used it for the synthesis of calixspherands,[1] calixcrowns,[2] water-soluble cyclodextrin−calix[4]arene host molecules,[3] holands,[4] and anion receptors.[5] Because of their well-known chemical and physical properties, building blocks like crown ethers,[6,7] cryptands,[6] calixresor[4]arenes,[8] cyclotriveratrylenes,[9] clefts,[10] cyclodextrins,[11] and calix[4]arenes[12] are used. In order to make calix[6]arenes available as suitable building blocks, we have systematically studied, in collaboration with the groups of Ungaro and de Mendoza, the selective lower[13] and upper rim functionalization.[14] Recently we demonstrated the three-point capping of *p-tert*-butylcalix[6]arene with cyclotriveratrylene in good yields,[15] and other groups reported the selective arylmethylation and aroylation,[16] selective alkylation,[17,18] bridging,[19] and capping[20] of *p-tert*-butylcalix[6]arene.

For potential applications of calix[6]arenes the understanding of their conformational and dynamic behavior is a prerequisite. Studies on the dynamics of calix[4]arenes have been described by van Loon *et al.*[21] and Groenen *et al.*[22] They showed that in calix[4]arenes all conformations, e.g., cone, partial cone, 1,2-alternate, and 1,3-alternate, may be involved in the conformational interconversion process. Recently, pinched cone inter-

† Laboratory of Organic Chemistry.
‡ Laboratory of Chemical Analysis.
§ Laboratory of Chemical Physics.
⊗ Abstract published in *Advance ACS Abstracts,* April 1, 1996.

(1) For a recent example see: Iwema Bakker, W. I.; Haas, M.; Beattie-Khoo, C.; Ostaszewski, R.; Franken, S. M.; den Hertog, H. J., Jr.; Verboom, W.; de Zeeuw, D.; Harkema, S.; Reinhoudt, D. N. *J. Am. Chem. Soc.* **1994**, *116*, 123.

(2) Casnati, A.; Pochini, A.; Ungaro, R.; Ugozzoli, F.; Arnaud, F.; Fanni, S.; Schwing, M.-J.; Egberink, R. J. M.; de Jong, F.; Reinhoudt, D. N. *J. Am. Chem. Soc.* **1995**, *117*, 2767 and references cited therein.

(3) van Dienst, E.; Snellink, B. H. M.; von Piekartz, I.; Engbersen, J. F. J.; Reinhoudt, D. N. *J. Chem. Soc., Chem. Commun.* **1995**, 1151.

(4) Timmerman, P.; Nierop, K. G. A.; Brinks, E. A.; Verboom, W.; van Veggel, F. C. J. M.; van Hoorn, W. P.; Reinhoudt, D. N. *Chem. Eur. J.* **1995**, *1*, 124.

(5) (a) Rudkevich, D. M.; Verboom, W.; Reinhoudt, D. N. *J. Org. Chem.* **1994**, *59*, 3683; (b) Visser, H. C.; Rudkevich, D. M.; Verboom, W.; de Jong, F.; Reinhoudt, D. N. *J. Am. Chem. Soc.* **1994**, *116*, 11554.

(6) Gokel, G. W. In *Crown Ethers and Cryptands*; Stoddart, J. F., Ed.; The Royal Society of Chemistry: Cambridge, 1991.

(7) Izatt, R. M.; Pawlak, K.; Bradshaw, J. S.; Bruening, R. L. *Chem. Rev.* **1991**, *91*, 1721.

(8) (a) Timmerman, P.; Verboom, W.; Reinhoudt, D. N. *Tetrahedron* **1996**, *52*, 2663. (b) Cram, D. J.; Cram, J. M. In *Container Molecules and their Guests*; Stoddart, J. F., Ed.; The Royal Society of Chemistry: Cambridge, 1994.

(9) (a) Collet, A. *Tetrahedron* **1987**, *43*, 5725; (b) Collet, A.; Dutasta, J.-P.; Lozach, B.; Canceill, J. *Top. Curr. Chem.* **1993**, *165*, 103.

(10) (a) Rebek, Jr., J. *Angew. Chem., Int. Ed. Engl.* **1990**, *29*, 245; (b) Hamilton, A. D. In *Advances in Supramolecular Chemistry*; Gokel, G. W., Ed.; JAI Press Inc.: London, 1990; Vol. 1, p 1.

(11) Szejtli, J. *Cyclodextrin Technology*; Kluwer Academic Press: Dordrecht, The Netherlands, 1988.

(12) For a recent review see: Böhmer, V. *Angew. Chem., Int. Ed. Engl.* **1995**, *34*, 713.

(13) Janssen, R. G.; Verboom, W.; Reinhoudt, D. N.; Casnati, A.; Freriks, M.; Pochini, A.; Ugozzoli, F.; Ungaro, R.; Nieto, P. M.; Carramolino, M.; Cuevas, F.; Prados, P.; de Mendoza, J. *Synthesis* **1993**, 380.

(14) (a) de Mendoza, J.; Carramolino, M.; Cuevas, F.; Nieto, P. M.; Prados, P.; Reinhoudt, D. N.; Verboom, W.; Ungaro, R.; Casnati, A. *Synthesis* **1994**, 47; (b) Casnati, A.; Domiano, L.; Pochini, A.; Ungaro, R.; Carramolino, M.; Magrans, J. O.; Nieto, P. M.; López-Prados, J.; Prados, P.; de Mendoza, J.; Janssen, R. G.; Verboom, W.; Reinhoudt, D. N. *Tetrahedron* **1995**, *51*, 12699.

(15) Janssen, R. G.; Verboom, W.; van Duynhoven, J. P. M.; van Velzen, E. J. J.; Reinhoudt, D. N. *Tetrahedron Lett.* **1994**, *35*, 6555.

(16) (a) Rogers, J. S.; Gutsche, C. D. *J. Org. Chem.* **1992**, *57*, 3152; (b) Kanamathareddy, S.; Gutsche, C. D. *J. Org. Chem.* **1992**, *57*, 3160.

(17) Otsuka, H.; Araki, K.; Shinkai, S. *J. Org. Chem.* **1994**, *59*, 1542.

(18) (a) Neri, P.; Pappalardo, S. *J. Org. Chem.* **1993**, *58*, 1048; (b) Neri, P.; Consoli, G. M. L.; Cunsolo, F.; Piattelli, M. *Tetrahedron Lett.* **1994**, *35*, 2795.

(19) (a) Kanamathareddy, S.; Gutsche, C. D. *J. Am. Chem. Soc.* **1993**, *115*, 6572; (b) Casnati, A.; Jacopozzi, P.; Pochini, A.; Ugozzoli, F.; Cacciapaglia, R.; Mandolini, L.; Ungaro, R. *Tetrahedron* **1995**, *51*, 591.

(20) (a) Takeshita, M.; Nishio, S.; Shinkai, S. *J. Org. Chem.* **1994**, *59*, 4032; (b) Araki, K.; Akao, K.; Otsuka, H.; Nakashima, K.; Inokuchi, F.; Shinkai, S. *Chem. Lett.* **1994**, 1251.

(21) van Loon, J.-D.; Groenen, L. C.; Wijmenga, S. S.; Verboom, W.; Reinhoudt, D. N. *J. Am. Chem. Soc.* **1991**, *113*, 2378.

(22) Groenen, L. C.; van Loon, J.-D.; Verboom, W.; Harkema, S.; Casnati, A.; Ungaro, R.; Pochini, A.; Ugozzoli, F.; Reinhoudt, D. N. *J. Am. Chem. Soc.* **1991**, *113*, 2385.

conversion in calix[4]arenes has been established.[23,24] In this dynamic process two pinched cones with C_{2v} symmetry rapidly interconvert. The transition state is supposed to be a "perfect" cone conformation with C_{4v} symmetry. Recently, we showed that the conformations of C_{3v} *p-tert*-butylcalix[6]arenes, which are alternately substituted with small alkyl and other (bulkier) substituents, are stabilized by the self-inclusion of the alkyl substituents, and macrocyclic ring interconversion can take place via two different pathways, *viz.*, "*p-tert*-butyl through the annulus" and *O*-substituent through the annulus".[25] That study reflected only one aspect of the more complicated dynamics of functionalized calix[6]arenes when compared to calix[4]arenes. However, the larger calix[6]arene skeleton also gives more rotational freedom to the methylene bridges. Moreover, the hydrogen bonds of partially substituted calix[6]arenes may be involved in hydrogen bond array reversal or hydrogen bond flip-flop.[26] This dynamic process is characterized by the change of direction of the hydrogen bonds between the phenolic hydroxyl groups and was proposed in the literature for calix[8]arene[27b] and partially substituted calix[4]arenes,[27a,c] although conclusive evidence was never obtained. Besides the above-mentioned publications, very few other systematic studies on dynamics and conformational studies on calixarenes by 2D NMR spectroscopy are known.[28,29] Pons *et al.* investigated the conformational and dynamic behavior of an upper rim substituted trichlorocalix[6]-arene.[29] On the basis of molecular modeling they concluded that this derivative adopts a winged cone conformation (two aryl groups in "out" alignments and the other four in "up" and/ or "down" positions[27b]) in solution. The observed dynamic processes were macrocyclic ring inversion, hydrogen bond array reversal,[30] and pseudorotation.[31] Hence, one can expect a complex overall dynamics for most calix[6]arenes due to the superposition of these different processes.

In this paper, we report a study on the *overall dynamics* of *p-tert*-butylcalix[6]arene (thio)phosphates **2−10**. Their ^{1}H NMR spectra are generally complex due to overlap or coalescence of characteristic signals. The ^{31}P nucleus, however, in these calix-[6]arene (thio)phosphates provides a convenient probe for observing conformational details and dynamic processes. The

Chart 1

	R_1	R_2	R_3	R_4	R_5	R_6
1	OH	OH	OH	OH	OH	OH
2	OPO(OEt)$_2$	OH	OH	OH	OH	OH
3	OPO(OEt)$_2$	OH	OPO(OEt)$_2$	OH	OH	OH
4	OPO(OEt)$_2$	OH	OH	OPO(OEt)$_2$	OH	OH
5	OPO(OEt)$_2$	OPO(OEt)$_2$	OH	OPO(OEt)$_2$	OH	OH
6	OPO(OEt)$_2$	OPO(OEt)$_2$	OPO(OEt)$_2$	OPO(OEt)$_2$	OPO(OEt)$_2$	OPO(OEt)$_2$
7	OPS(OEt)$_2$	OH	OH	OH	OH	OH
8	OPS(OEt)$_2$	OH	OPS(OEt)$_2$	OH	OH	OH
9	OPS(OEt)$_2$	OH	OH	OPS(OEt)$_2$	OH	OH
10	OPS(OEt)$_2$	OPS(OEt)$_2$	OPS(OEt)$_2$	OPS(OEt)$_2$	OPS(OEt)$_2$	OH

combined details from these studies provide for the first time information about the complex relation between different substitution patterns and the concomitant occurrence of distinct dynamic processes in calix[6]arenes. Furthermore, the results in this paper illustrate how multinuclear NMR spectroscopy can be used as a powerful tool to unravel complicated dynamic processes. The methodology described may well be applied to other calix[*n*]arenes and related macrocycles.

Results and Discussion

Synthesis of (Thio)phosphates 2−10. The *p-tert*-butylcalix-[6]arene phosphates **2−6** (Chart 1) have been prepared by reaction of *p-tert*-butylcalix[6]arene (**1**) with diethoxyphosphoryl chloride in the presence of varying amounts of Et$_3$N as a base in refluxing chloroform and have been described by us in a preliminary communication.[32] Details of the synthesis are presented in the Experimental Section. Thiophosphorylated calix[6]arenes **7−10** (Chart 1) have been described in detail (see ref 33).

Solid State Structures of the Thiophosphates 7 and 9. Recrystallization of mono(thiophosphate) **7** from acetonitrile yielded high-quality single crystals suitable for X-ray diffraction. The X-ray crystal structure shows that mono(thiophosphate) **7** adopts a slightly distorted pinched cone conformation in which the calix[6]arene skeleton is pinched around two distal methylene bridges in the same fashion as was observed in the case of *p*-alkylcalix[6]arenes[34] (Figure 1). One acetonitrile molecule is intercalated in a void between two calix[6]arenes, but is not included in the open disklike cavity, which is formed by the six aromatic moieties. From difference Fourier maps, all hydrogen atoms of the phenolic hydroxyl groups could be located, which is to the best of our knowledge one of the very few examples in calixarene chemistry. The five hydroxyl groups together form a hydrogen bond array (Table 1). Four hydrogen bonds (involving H51, H71, H91, and H111) are almost linear; one (involving H31) is bifurcated.

Taking into account both the criteria of minimal bond angle as well as maximal O···O distance, both contacts involving H31 can be classified as hydrogen bonds,[35] and form a so-called

(23) (a) Yamada, A.; Murase, T.; Kikukawa, K.; Arimura, T.; Shinkai, S. *J. Chem. Soc.*, *Perkin Trans. 2* **1991**, 793; (b) Conner, M.; Janout, V.; Regen, S. L. *J. Am. Chem. Soc.* **1991**, *113*, 9670; (c) Arduini, A.; Fanni, S.; Manfredi, G.; Pochini, A.; Ungaro, R.; Sicuri, A.-R.; Ugozzoli, F. *J. Org. Chem.* **1995**, *60*, 1448.

(24) On the basis of relaxation time measurements of calix[*n*]arene esters and their Na$^+$ complexes in ref 23a, a similar interconversion process was suggested for calix[6]arenes. In the case of calix[4]arenes, macrocyclic ring inversion is blocked by the substituents and decrease of the relaxation times can be attributed to a suppression of the "seesaw" motion of the calix-[4]arene skeleton by the template effect of the Na$^+$ ion. However, the calix-[6]arene ester shows macrocyclic ring inversion, which is also suppressed by complexation. Hence, these experiments do not prove a seesaw motion for calix[6]arenes, although such a movement might also be possible.

(25) van Duynhoven, J. P. M.; Janssen, R. G.; Verboom, W.; Franken, S. M.; Casnati, A.; Pochini, A.; Ungaro, R.; de Mendoza, J.; Nieto, P. M.; Prados, P.; Reinhoudt, D. N. *J. Am. Chem. Soc.* **1994**, *116*, 5814.

(26) Koehler, J. E. H.; Saenger, W.; van Gunsteren, W. F. *Eur. Biophys. J.* **1988**, *16*, 153.

(27) Grootenhuis, P. D. J.; Kollman, P. A.; Groenen, L. C.; Reinhoudt, D. N.; van Hummel, G. J.; Ugozzoli, F.; Andreetti, G. D. *J. Am. Chem. Soc.* **1990**, *112*, 4165; (b) Gutsche, C. D.; Bauer, L. J. *J. Am. Chem. Soc.* **1985**, *107*, 6052; (c) Groenen, L. C.; Steinwender, E.; Lutz, B. T. G.; van der Maas, J.; Reinhoudt, D. N. *J. Chem. Soc.*, *Perkin Trans. 2* **1992**, 1893.
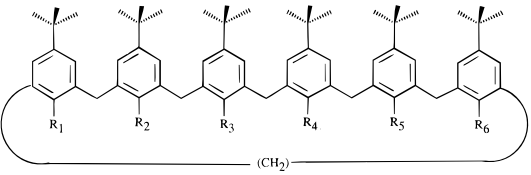
(28) Hofmeister, G. E.; Alvaro, E.; Leary, J. A.; Yoon, D. I.; Pedersen, S. F. *J. Am. Chem. Soc.* **1990**, *112*, 8843.

(29) Molins, M. A.; Nieto, P. M.; Sanchez, C.; Prados, P.; de Mendoza, J.; Pons, M. *J. Org. Chem.* **1992**, *57*, 6924.

(30) Hydrogen bond array reversal is a process in which the cyclic hydrogen bond array reverses its directionality from a clockwise to a counterclockwise direction either by breaking the hydrogen bonds sequentially or by a tunneling mechanism.

(31) *Pseudo*rotation is referred to as the process in which the macrocyclic ring "folds" and places alternately two distal aromatic moieties in an "out" position. All atoms are thus *virtually* rotated over an angle of 120°.

(32) Janssen, R. G.; Verboom, W.; Harkema, S.; van Hummel, G. J.; Reinhoudt, D. N.; Pochini, A.; Ungaro, R.; Prados, P.; de Mendoza, J. *J. Chem. Soc.*, *Chem. Commun.* **1993**, 506. Recently our results have been independently confirmed: Regnouf de Vains, J.-B.; Pellet-Rostaing, S.; Lamartine, R. *Tetrahedron Lett.* **1994**, *35*, 8147.

(33) Wroblewski, W.; Brzozka, Z.; Janssen, R. G.; Verboom, W.; Reinhoudt, D. N. *New J. Chem.*, in press.

(34) See for instance: Andreetti, G. D.; Ugozolli, F.; Casnati, A.; Ghidini, E.; Pochini, A.; Ungaro, R. *Gazz. Chim. Ital.* **1989**, *119*, 47.

(35) Jeffrey, G. A.; Saenger, W. *Hydrogen Bonding in Biological Structures*; Springer-Verlag: Berlin, Heidelberg, 1991.
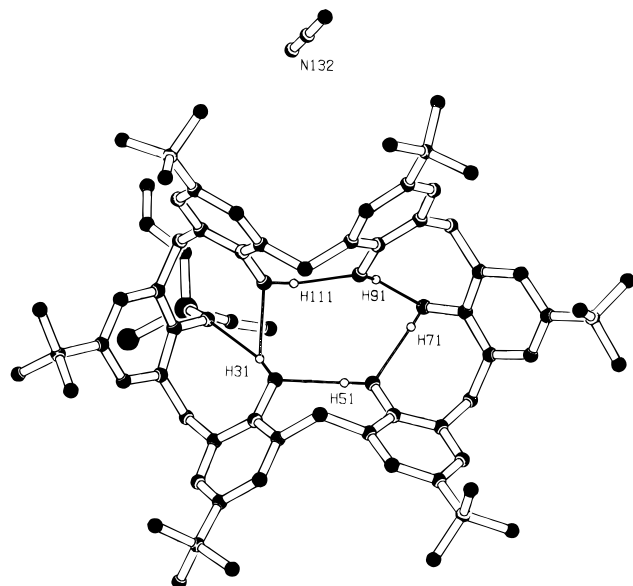
Figure 1. Solid-state structure of mono(thiophosphate) **7**. Geometrical parameters are displayed in Table 1.

Table 1. Hydrogen Bond Distances (Å) and Angles (deg) in Mono(thiophosphate) **7**[a]

atoms	d_{O-H}	$d_{H \cdots O}$	$d_{O \cdots O}$	angle$_{O-H \cdots O}$
O31−H31···O11	0.74(6)	2.59(5)	3.094(5)	127(6)
O31−H31···O111	0.74(6)	2.30(6)	2.897(6)	139(5)
O51−H51···O31	0.80(4)	1.95(4)	2.742(4)	174(6)
O71−H71···O51	0.68(3)	2.02(3)	2.667(4)	160(4)
O91−H91···O71	0.73(4)	2.02(4)	2.732(6)	167(3)
O111−H111···O91	0.85(4)	1.88(3)	2.720(4)	170(4)

[a] The atomic numbering scheme is depicted in Figure 1.

three-centered hydrogen bond structure with the *medial*[36] hydrogen bond H31···O111 as the *major* component. The cyclic character of the hydrogen bond array of the unsubstituted *p-tert*-butylcalix[6]arene is thus partially maintained, which is energetically favorable. The previously reported solid state structure of 1,4-bis(thiophosphate) **9**[32] exhibits the same conformational features as mono(thiophosphate) **7** in adopting a pinched cone structure. The molecule has a C_2 axis of symmetry, and the folded structure gives the molecule a disklike shape. The O···O distance between two medially positioned hydroxyl groups is 2.98 Å, and the shortest O···O distance between a hydroxyl group and the phenolic oxygen atom of a thiophosphorylated moiety is 2.83 Å. These distances are, respectively, slightly longer and significantly shorter than in the case of mono-(thiophosphate) **7** (2.90 and 3.10 Å, respectively). Both medial and proximal hydrogen bonds form an array with a partially cyclic character. This means that pinching is a favorable process, because it would provide a way to combine short hydrogen bonds and optimal alignment between proximal hydroxyl groups, while the three-centered hydrogen bonds between medially positioned hydroxyl groups preserve the *cyclic* nature of the hydrogen bond array.

Structure Elucidation and Dynamics in Solution of the Phosphates 2−4 and Thiophosphates 7−9. In order to investigate the conformations and dynamics in solution of the (thio)phosphorylated *p-tert*-butylcalix[6]arenes **2−4** and **7−9**, these compounds were subjected to variable-temperature NMR spectroscopy. ^{1}H and ^{31}P NMR spectra of phosphates **2−4** and thiophosphates **7−9** were recorded at 193 K in CD$_2$Cl$_2$[37] and

between 213 and 333 K in CDCl$_3$ for the phosphates **2−4** and in CD$_2$Cl$_2$ for the thiophosphates **7−9**.

The spectra of phosphates **2−4** are depicted in Figure 2. Important spectral data are displayed in Table 2. Information about the structures and dynamics was obtained from ^{1}H NOESY/EXSY, ROESY, and TOCSY spectra. Further information concerning dynamic processes was derived from ^{31}P EXSY spectroscopy and $T_{1\rho}$ measurements. The next section is subdivided in three paragraphs, each one dealing with (thio)-phosphates with the same substitution pattern.

Monophosphate 2 and Mono(thiophosphate) 7. At room temperature the ^{1}H NMR spectra of both monophosphate **2** and mono(thiophosphate) **7** in CDCl$_3$ and CD$_2$Cl$_2$ exhibit three AX spin systems for the methylene protons and four signals for the *tert*-butyl protons in the ratio 1:1:1 and 1:1:2:2, respectively, while the ^{31}P NMR spectra of both compounds exhibit a single resonance. Upon cooling of monophosphate **2**, the signals of two AX spin systems of the methylene bridges become broad at 273 K, while the signals of the AX spin system with the largest $\Delta\delta$ (Table 2, Figure 2A) are still sharp. The ^{31}P NMR signal shows some line broadening, and at 243 K it decoalesces in two signals. The AX spin systems and hydroxyl resonances of the ^{1}H NMR spectrum decoalesce in multiple resonances. At 193 K, the ^{1}H NMR spectrum of monophosphate **2** exhibits multiple broad signals for the hydroxyl protons. The aromatic signals are sharp, while the methylene protons appear as multiple sets of AX spin systems. The ^{31}P NMR spectrum clearly shows two signals in the ratio 2:1, from which it can be concluded that at least two conformers are present in solution. The TOCSY spectrum of monophosphate **2** at 193 K exhibits three AX spin systems of equally strong intensity, which were assigned to a low-energy (major) conformer, and six AX spin systems of equally weak intensity, which were assigned to a second (minor) conformer. The ^{1}H NMR spectrum of mono(thiophosphate) **7** slightly broadened upon cooling to 193 K, and only the signals of the hydroxyl protons decoalesced in multiple resonances, but no minor conformer could be observed. The ^{31}P NMR spectrum at 193 K exhibits a single resonance, and the possibility that it is the average of two signals like those of monophosphate **2** was ruled out with a ^{31}P $T_{1\rho}$ vs ω_1 experiment.[38] The throughout nondegenerate state of the signals of the axial and equatorial methylene bridge protons of the conformers of monophosphate **2** and mono(thiophosphate) **7** in the temperature interval between 193 and 333 K indicates that macrocyclic ring interconversion in this temperature interval is still slow on the chemical shift time scale.[39] The coalescence of the AX spin systems of the major and minor conformer of monophosphate **2** to a new, *averaged* AX spin system at the lowest coalescence temperature should thus be ascribed to *other* dynamic processes than flipping of aromatic moieties through the calix[6]arene annulus. Due to this averaging, the exchange connectivity between the signals of the equatorial and the axial protons of the AX spin system of a NOESY spectrum recorded above the highest coalescence temperature can only be attributed to macrocyclic ring interconversion. The corresponding activation Gibbs free energies ($\Delta G_m^{\ddagger}$) of 77 and 86 kJ·mol^{-1} (Table 3) for monophosphate **2** and mono(thiophosphate) **7**, respectively, were calculated using the initial rate approximation. The NOESY spectrum of monophosphate **2** at 193 K showed strong NOE connectivities between the signals of the equatorial (upfield) methylene protons and those of the aromatic ones of both the major and the minor

(36) "Proximal" are two aromatic moieties, which are connected directly via a methylene bridge; "medial" are two aromatic moieties, which are separated by one other aromatic moiety; "distal" are two aromatic moieties, which are separated by two other aromatic moieties.

(37) As CDCl$_3$ freezes at 210 K, measurements were performed in CD$_2$-Cl$_2$ in order to detect low-barrier interconversion processes.

(38) Wang, Y.-S.; Ikuta, S. *Magn. Reson.* **1989**, *27*, 1134.

(39) Fast macrocyclic ring interconversion degenerates the signals of the AX spin systems to singlets.
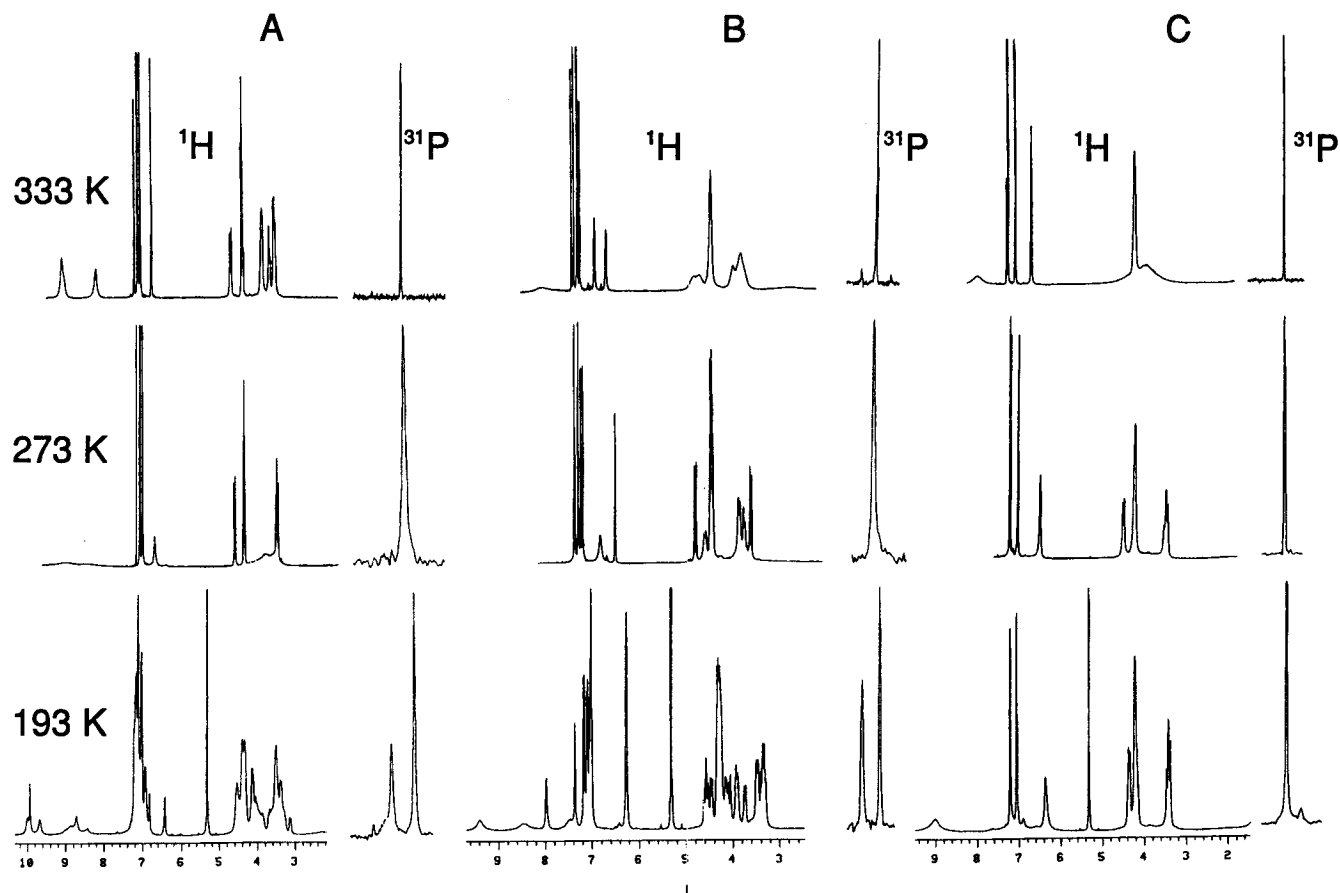
Figure 2. Variable-temperature ^{1}H and ^{31}P NMR spectra of monophosphate **2** (A), 1,3-diphosphate **3** (B), and 1,4-diphosphate **4** (C).

Table 2. ^{1}H NMR Data of *p-tert*-Butylcalix[6]arene Phosphates **2−4** and Thiophosphates **7−9**

compd	T (K)	$\delta_{AX}{}^a$	$\Delta\delta_{AX}$	$\delta_{OH}{}^a$	compd	T (K)	$\delta_{AX}{}^a$	$\Delta\delta_{AX}$	$\delta_{OH}{}^a$
2	193	4.54/3.50 (A,E)$_{2/3}$	1.04	6.90/8.70 (a)	**3**		4.56/3.46 (A,E)$_5$	1.10	
major		4.02/3.36 (A,E)$_{1/4}$	0.66	9.60/10.0 (b)			4.46/3.34 (A,E)$_6$	1.12	
		4.14/3.50 (A,E)$_{5/6}$	0.64	9.90 (c)		303	4.68/3.54	1.14	
minor		3.70/3.10	0.6	9.0−8.0			4.52/3.70	0.82	8.6−8.0
		3.90/3.40	0.5				3.81/3.64	0.17	
		3.90/3.30	0.6		**8**	193	3.68/3.36 (A,E)$_{1/2}$	0.50	7.8/7.3 (a)
		4.00/3.30	0.7				3.74/3.32	0.42	9.4 (b)
		4.50/3.60	0.9				4.23/3.57 (A,E)$_{3/4}$	0.66	
		4.50/3.45	1.05				4.02/3.76	0.26	
	303	4.70/3.57	1.13	9.4−9.1			4.23/3.57 (A,E)$_{5/6}$	0.66	
		3.87/3.67	0.20	8.5−8.1			4.23/3.57	0.66	
		3.87/3.54	0.33			303	4.50/3.65	0.85	
7	193−303	4.66/3.59	1.07	10.0, 9.9,			4.35/3.70	0.65	
		4.20/3.67	0.63	9.7, 8.8			3.75/3.70	0.05	
		3.87/3.54	0.54		**4**	193	4.35/3.35	1.0	9.0
3	193	3.92/3.38 (A,E)$_1$	0.54	8.0/7.4 (a)			4.10/3.40	0.70	
		3.74/3.32 (A,E)$_2$	0.42	9.5 (b)	**9**	303	4.57/3.49	1.08	7.0
		4.58/3.50 (A,E)$_3$	1.08	8.4 (c)			3.93/3.39	0.54	
		4.06/3.90 (A,E)$_4$	0.16						

^{a} (Pairs of) AX spin systems (axial and equatorial methylene bridge protons) are indicated with (A,E)$_i$; (pairs of) hydroxyl resonances are indicated with a, b, and c.

conformers, which unequivocally points to a *syn*-orientation of the aromatic moieties.

Additionally, a through-space/through-bond walk via the signals of the aromatic protons and the equatorial methylene protons of a ROESY spectrum recorded above the lowest coalescence temperature is in line with an averaged *syn*-conformation. From the intensity ratios of the AX spin systems and the *tert*-butyl groups, it is concluded that the major *syn*-conformer has a pseudo plane of symmetry[40] (pseudo-C_s symmetry) (Table 4). The six AX spin systems of the minor conformer point to an asymmetrical *syn*-arrangement of the aromatic moieties.

Hydrogen Bond Array Reversal. The hydroxyl protons **a**

at 6.90 and 8.70 ppm (Table 2) exhibit a strong exchange connectivity, which was also observed for the hydroxyl protons **b** at 9.60 and 10.0 ppm. Between the hydroxylic protons **a−c** and the signals of the axial (downfield) methylene protons of the major conformer, NOE connectivities were observed. These spectral features are in accordance with a hydrogen bond array, which switches between a clockwise and a counterclockwise directionality[41] and is formed by all hydroxyl groups. The lone

(40) A pseudosymmetry element is a hypothetic "spectroscopically" observed symmetry element, which is the result of averaging of signals by fast exchange of conformers. Pseudosymmetry elements are also assigned to nearly symmetrical structures, of which the symmetry-related groups cannot be spectroscopically distinguished.

Table 3. Thermodynamic and Kinetic Data of Phosphates **2−4** and Thiophosphates **7−9**

compd	ΔG^a (kJ·mol^{-1})	hydrogen bond array reversal, $\Delta G_h^{\ddagger\,g}$ (kJ·mol^{-1})	pinched conformer interconversion, $\Delta G_p^{\ddagger\,c,h}$ (kJ·mol^{-1})	macrocyclic ring interconversion, $\Delta G_m^{\ddagger\,b,i}$ (kJ·mol^{-1})
2	2.2	44^{b,c}	48	77
3	0	e	45	69
4	4.3	31^d	55	67
7	f	45^b	f	86^j
8	0	e	44	73
9	f	<31^d	f	73

^{a} Calculated from the intensity ratio of the phosphorous signals at 193 K. ^{b} Calculated from ^{1}H exchange connectivities. ^{c} Calculated from ^{31}P exchange connectivities. ^{d} Calculated from ^{1}H $T_{1\rho}$ measurements. ^{e} Only qualitative ^{31}P $T_{1\rho}$. ^{f} No minor conformer observed. ^{g} Measured at 193 K. ^{h} Measured at 223 K. ^{i} Measured at 303 K. ^{j} Measured at 328 K.

Table 4. Theoretical ^{1}H NMR Intensity Ratios for Mono- and Disubstituted *syn*-Structures with a (pseudo)-C_s Symmetry^a

| substitution pattern	no. of AX spin systems	no. of *tert*-butyl groups
mono	3 (1:1:1)	4 (1:1:2:2)
1,2-di	4 (1:1:2:2)	3 (1:1:1)
1,3-di	3 (1:1:1)	4 (1:1:2:2)
1,4-di	2 (1:2)	2 (1:2)

^{a} Relative intensities are given in parentheses.

pair of the phosphorylated phenolic oxygen atom is supposed to accept the terminal hydrogen bond of the hydrogen bond array, by which the phosphate group is oriented asymmetrically. Due to a combination of low spectral resolution and small chemical shift differences, the AX spin systems of pseudo-C_s-symmetry-related methylene bridges cannot be distinguished separately. Hence, only three pairs of AX spin systems and three *tert*-butyl groups are observed for the major conformer. Due to the downfield shift of protons involved in strong cooperative hydrogen bonding, terminal and initial hydroxyl groups of a hydrogen bond array should be more upfield shifted than those in the central part of the hydrogen bond array. The downfield shift of the **a** proton at 8.7 ppm compared to the proton at 6.9 ppm is attributed to cooperativity, and therefore the proton at 8.7 ppm is assigned to the hydroxyl group which terminates the hydrogen bond array, while the proton at 6.9 ppm is assigned to the hydroxyl group which initiates the hydrogen bond array.

Proton **c** at 9.9 ppm (Table 2) exhibits no exchange connectivity, which shows that for both directionalities of the hydrogen bond array it has the same magnetic environment. It is therefore necessarily located at the distal position relative to the phosphate group (with the oxygen atom located in the pseudo-σ-plane[40]). Assignment of the other AX spin systems and hydroxylic signals was performed in a straightforward manner by scrutiny of the NOE and exchange connectivities. The complete assignment is depicted in Figure 3. Activation Gibbs free energies for hydrogen bond array reversal ($\Delta G_h^{\ddagger}$) of 44 and 45 kJ·mol^{-1} for monophosphate **2** and mono-(thiophosphate) **7**, respectively (Table 3), were calculated straightforwardly from the exchange connectivities between the signals of the phenolic hydroxyl groups.

Pinched Conformer Interconversion. In the solid state, mono(thiophosphate) **7** adopts a pinched cone conformation (*vide supra*). This folding of the calix[6]arene skeleton optimizes the hydrogen bond angles and distances, and stabilizes

(41) Both conformers, which only differ with respect to directionality through the conformational orientation of chemical groups, are called cycloenantiomers.
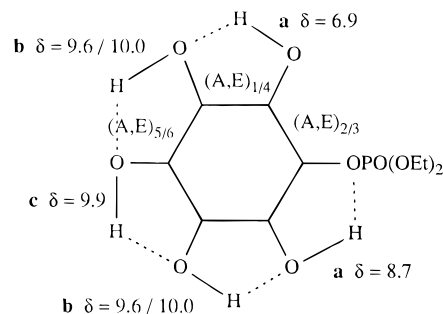
Figure 3. Assignment of signals to the different hydroxylic protons and axial (A) and equatorial (E) methylene bridge protons of monophosphate **2**. Each corner represents a phenolic moiety.
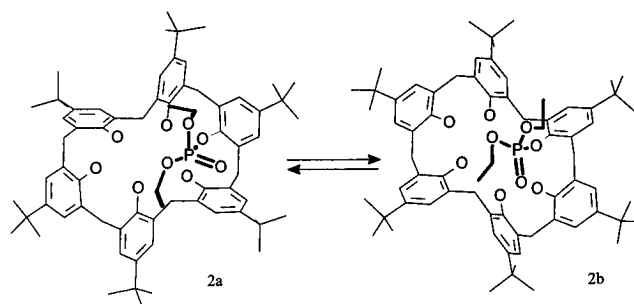
Figure 4. Pinched conformer interconversion between major (**2a**) and minor (**2b**) pinched conformers of monophosphate **2**.

the conformation. Moreover, different pinched structures are possible for substituted calix[6]arenes which explains the presence of a major and a minor conformer of monophosphate **2**. The major conformer **2a** is, like the solid state structure, pinched as depicted in Figure 4 and obeys the pseudo-C_s symmetry relation as observed in the ^{1}H NMR spectrum.

The minor conformer is postulated to be structure **2b** as depicted in Figure 4.[42] According to space-filling CPK molecular models, this folding also results in a strong hydrogen bond array, although the structure seems slightly more strained.

In both structures **2a** and **2b**, the phosphate group is in different magnetic environments, which explains the ^{31}P NMR spectra very well. In principle four pinched structures for **2b** can be derived: two pairs that are mirror images (Figure 5), and thus have equal Gibbs free energies. A difference in Gibbs free energy of 2.2 kJ·mol^{-1} (Table 3) between both the major and minor conformers was calculated from the intensity ratios of the ^{31}P NMR signals. Interconversion between both conformers does not destroy the *syn*-arrangement and involves the *rotation of a methylene bridge from pointing inside the calix-[6]arene annulus to a position pointing toward the exterior*. This interconversion process is defined as *pinched conformer interconversion* (Figure 4). The exchange connectivity between both ^{31}P signals solely originates from this process and is not obscured by other dynamic processes. An activation Gibbs free energy ($\Delta G_p^{\ddagger}$) of 48 kJ·mol^{-1} was calculated (Table 3) using the initial rate approximation. Pinched conformer interconversion between major and minor conformers according to the process depicted in Figure 5 gives rise to exchange of two pairs of protons of the methylene bridges as displayed in the scheme of Figure 6.

Scrutiny of the NOESY spectrum showed the presence of at least one exchange connectivity between the signal of an equatorial methylene proton of the minor conformer and that of an axial methylene proton of the major conformer, which

(42) Modeling shows that the distance between equatorial protons in an "inwardly" (pinched) or "outwardly" pointing methylene bridge with nearby aromatic protons is nearly the same, which makes discrimination between these structure elements based on distances calculated from NOEs impossible.
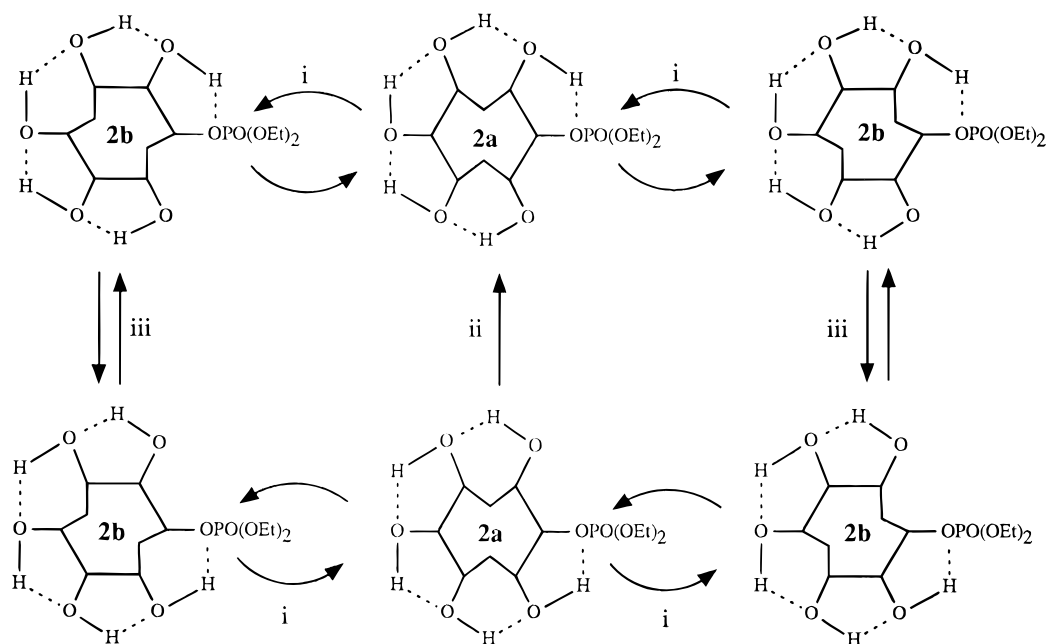
Figure 5. Pinched conformer interconversion pathways between major (**2a**) and minor (**2b**) pinched conformers (i). Routes ii and iii depict hydrogen bond array reversal in the major and minor conformers, respectively.
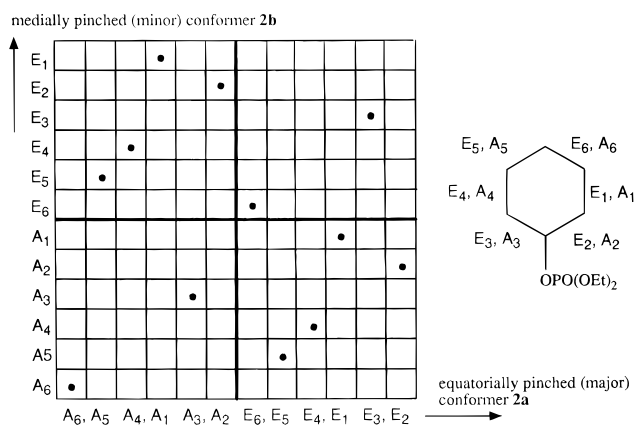

Figure 6. EXSY connectivity diagram of signals between the axial (A) and equatorial (E) methylene bridge hydrogens for the pinched conformer interconversion of monophosphate **2**. Nearly nondegenerate methylene protons of the major conformer (**2a**) are presented pairwise.

unambiguously supports the proposed interconversion of pinched conformers. However, due to overlap not all exchange connectivities could be located, and a complete assignment of the methylene signals of the minor conformer **2b** by tracking the exchange connectivities with already assigned signals of the major conformer **2a** was not possible.

1,3-Diphosphate 3 and 1,3-Bis(thiophosphate) 8. At ambient temperature the ^{1}H NMR spectra of both 1,3-phosphate **3** and 1,3-bis(thiophosphate) **8** exhibit three AX spin systems and four signals for the *tert*-butyl groups in the intensity ratio 1:1:1 and 1:1:2:2, respectively. The ^{1}H NMR spectrum of 1,3-diphosphate **3** exhibits some line broadening and starts to coalesce on increasing the temperature, while the signals of 1,3-bis(thiophosphate) **8** remain sharp. In a similar way, as described for the mono(thio)phosphates, activation Gibbs free energies for macrocyclic ring inversion of 69 and 73 kJ·mol^{-1} were calculated from the exchange connectivities between the signals of the axial and equatorial protons of 1,3-diphosphate (**3**) and 1,3-bis(thiophosphate) **8**, respectively (Table 3). Upon cooling of 1,3-diphosphate **3**, like for monophosphate **2**, two AX spin systems start to broaden at 273 K, while the AX spin system with the largest $\Delta\delta$ broadens at 243 K (Figure 2B). At the same temperature the single signal in the ^{31}P NMR spectrum

decoalesces in two broad signals. At 193 K, the ^{1}H NMR spectrum exhibits multiple AX spin systems for the methylene protons, while the hydroxyl groups appear as three broad and one sharp signal. The TOCSY spectrum at 193 K exhibits six AX spin systems for the methylene protons. Similarly to that for mono(thio)phosphates **2** and **7**, the NOESY spectrum at this temperature shows strong connectivities between the signals of the equatorial protons of the AX spin systems of the methylene bridges and the signals of the aromatic protons, which indicates the conformation to have *syn*-arranged aromatic rings. The ^{31}P NMR spectrum at 193 K exhibits two signals of equal intensity, but with clearly different line widths. The ^{31}P $T_{1\rho}$ values measured for the respective resonances revealed a clearly different dependency on the radiofrequent field strength, ω_1. From this observation it was deduced that each ^{31}P signal is the average of at least two other ^{31}P signals. Obviously both phosphate groups are not symmetry related, and 1,3-diphosphate **3** adopts a nonsymmetrical conformation with either a clockwise- or -counterclockwise-directed hydrogen bond array. Both orientations of the hydrogen bond array leave the phosphate groups in a different magnetic environment, and fast hydrogen bond array reversal leads to the observed averaged ^{31}P NMR signals. In analogy with the monophosphate **2**, a pinched cone conformation is in accordance with these spectral features. This was further supported by scrutiny of the NOESY spectrum, which, in addition to the NOEs between the signals of the axial and equatorial protons of the methylene bridges, also exhibits exchange connectivities between equatorial and equatorial protons and equatorial and axial protons. This indicated that the pinched cone conformers are involved in pinched conformer interconversion (Figure 7). Due to the equal sign of nuclear Overhauser and exchange effects in NOESY spectroscopy under these conditions, assignments in the methylene region were complicated. For this reason a ROESY spectrum was recorded (Figure 8), which enabled us to separate nuclear Overhauser from exchange effects by their different signs. Perusal of all ROE, NOE, and exchange connectivities, with the help of the EXSY connectivity diagram depicted in Figure 9, evolved pairs of exchanging methylene bridges for a monopinched conformer, and their relative positions.[43]

Although the OH groups are involved in fast hydrogen bond array reversal (Figure 7), each OH group has only one NOE
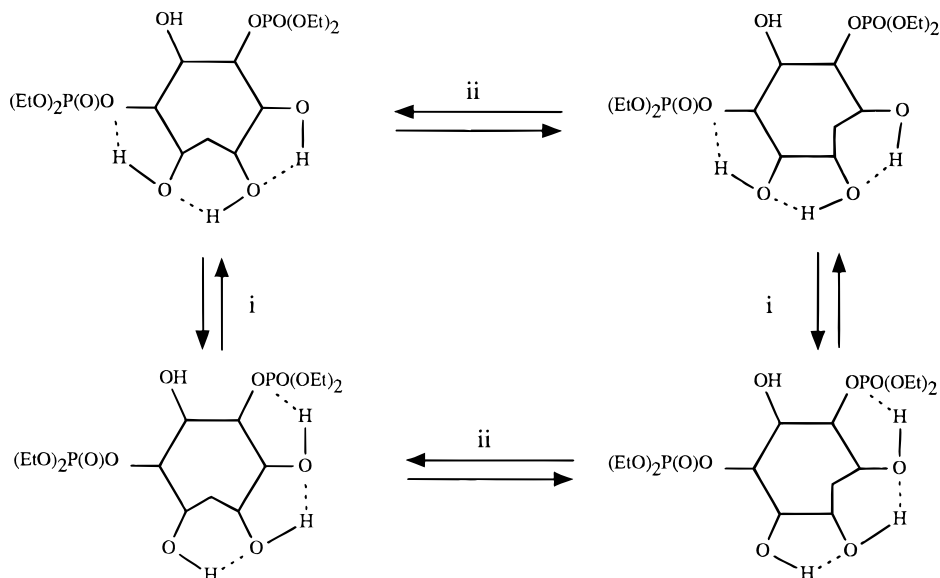
Figure 7. Hydrogen bond array reversal (i) and pinched conformer interconversion (ii) in 1,3-diphosphate **3**.
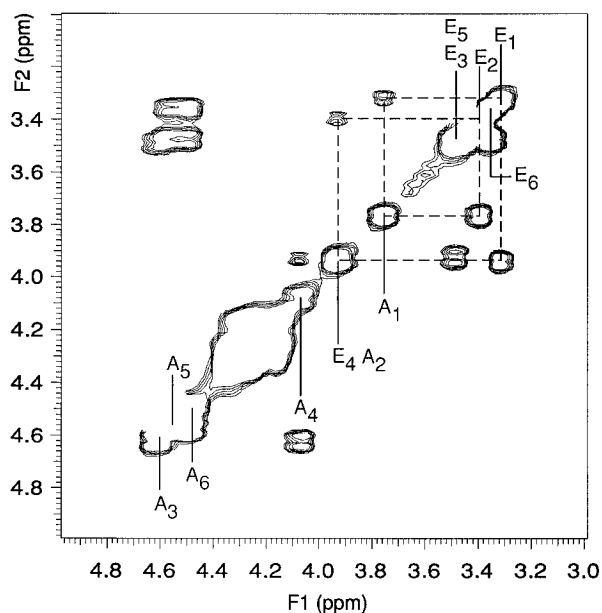

Figure 8. ROESY spectrum of 1,3-diphosphate **3** recorded at 193 K. Above the diagonal (negative) ROE connectivities and under the diagonal (positive) exchange connectivities are depicted between axial (A) and equatorial (E) methylene bridge protons.

Figure 9. EXSY connectivity diagram for the pinched conformer interconversion processes in 1,3-diphosphate **3** as depicted in Figure 7. A and E denote axial and equatorial methylene bridge protons, respectively.

connectivity with one axial proton of a methylene bridge, which points to a preferred orientation of the hydrogen bond array. The exchange connectivity between the hydroxyl groups located at 7.4 and 8.0 ppm supports the exchange pathways depicted in Figure 7. The calculated activation Gibbs free energies nicely matched those values obtained from the ^{31}P EXSY spectra (see Table 3). At room temperature the combination of hydrogen bond array reversal and pinched conformer interconversion thus gives rise to an averaged *syn*-conformation with pseudo-C_s symmetry, which was confirmed by a ROESY spectrum. The activation Gibbs free energies for pinched conformer interconversion for 1,3-diphosphate **3** and 1,3-bis(thiophosphate) **8** are 45 and 44 kJ·mol^{-1}, respectively (Table 3), which were calculated from the exchange connectivity between both ^{31}P NMR signals at 223 K.

(43) In fact, also a dipinched conformer might be possible; the methylene bridges (E,A)$_{5/6}$ should then be averaged by a much faster pinched conformer interconversion than that of the methylene bridges (E,A)$_{1/2}$. However, the difference in interconversion rate cannot be easily explained. More insight in this case might be obtained from high-level molecular modeling calculations.
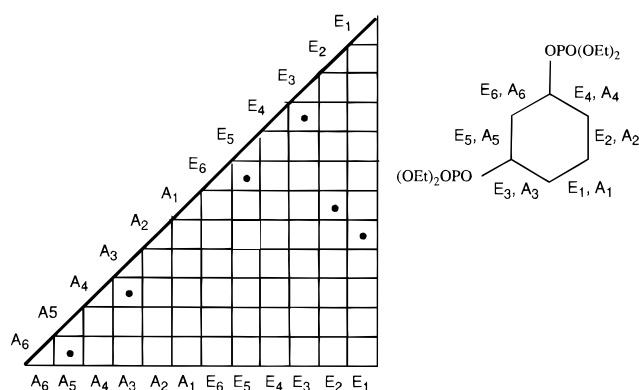
1,4-Diphosphate 4 and 1,4-Bis(thiophosphate) 9. All ^{1}H NMR signals of the methylene region of 1,4-diphosphate **4** are broad at room temperature, while those of 1,4-bis(thiophosphate) **9** are sharp. Upon cooling, the ^{1}H NMR spectra exhibit two sharp AX spin systems for the methylene bridges and two signals for the *tert*-butyl groups, both in the ratio 2:1. In a way similar to that described for the other compounds, activation Gibbs free energies for macrocyclic interconversion of 67 and 73 kJ·mol^{-1} were calculated at ambient temperature. For both phosphates a *syn*-conformation was deduced from a combined NOESY/TOCSY (through-space and through-bond walk) along the signals of the equatorial and aromatic protons. The ^{31}P NMR spectrum at 193 K of 1,4-diphosphate **4** exhibits one sharp signal for the phosphate group. In analogy with mono(thio)-phosphates **2** and **7**, and supported by the solid state structure of 1,4-bis(thiophosphate) **9** (*vide supra*), a pinched structure is proposed in solution too. In addition, close inspection of the ^{31}P NMR spectrum reveals a very small signal of a minor conformer, while minor conformer signals were as well observed in the ^{1}H NMR spectra below 243 K (Figure 2C). In the spectra of 1,4-bis(thiophosphate) **9** no minor conformer signals were observed. ^{31}P EXSY NMR spectra of 1,4-diphosphate **4** showed a connectivity between both signals, and in analogy with the former (thio)phosphates, it is supposed that this interconversion process comprises pinched conformer interconversion between the conformers **4a** and **4b** (Figure 10). Calculation of the Gibbs free energy of activation gave a value of 55 kJ·mol^{-1} (Table
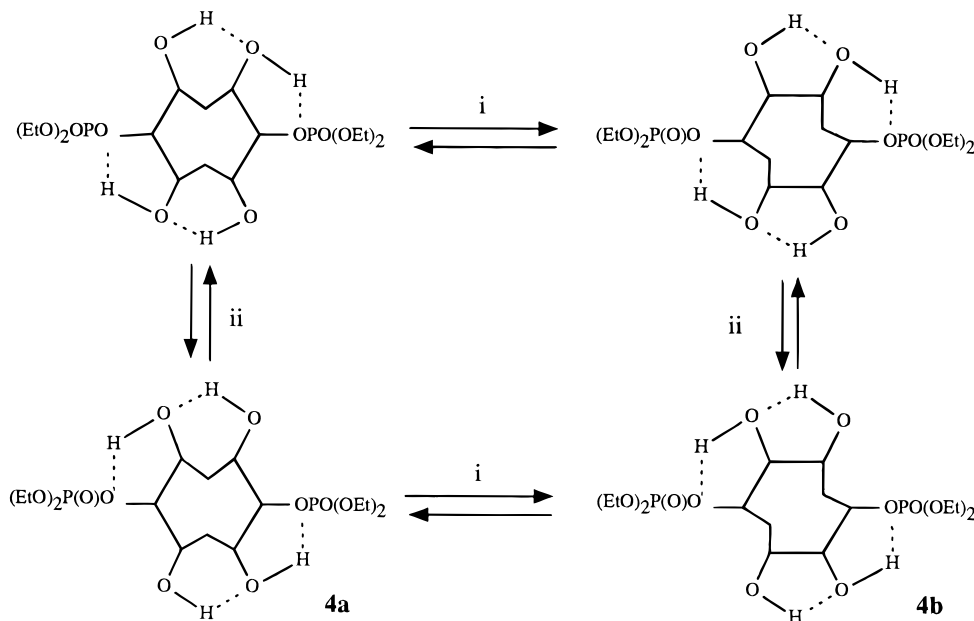
Figure 10. Pinched conformer interconversion (i) and hydrogen bond array reversal (ii) in 1,4-diphosphate **4**.

3). By the directionality of the hydrogen bond array, pinched conformer **4a** exhibits C_2 symmetry, and three AX systems for the methylene bridges should be observed. However, by fast hydrogen bond reversal, the symmetry becomes pseudo-C_s and both AX spin systems of the methylene bridges proximal to the phosphate group become averaged. From the dependence of ^1H $T_{1\rho ex}$ from the ω_1 field strength, it was deduced that the activation Gibbs free energy for hydrogen bond reversal is on the order of 31 kJ·mol^{-1} (Table 3). A Gibbs free energy difference between the pinched cone conformers of 4.3 kJ·mol^{-1} (Table 3) was calculated from the intensity ratios of the ^{31}P NMR signals, in the same way as for monophosphate **2**.

Discussion

Macrocyclic Ring Interconversion. The NMR data of monophosphate **2** and mono(thiophosphate) **7** show that the activation Gibbs free energy for macrocyclic ring interconversion is larger than that of unsubstituted *p-tert*-butylcalix[6]arene by 23 and 33 kJ·mol^{-1}, respectively. Upon introduction of a second phosphate or thiophosphate group the activation Gibbs free energy is still significantly larger than that for the unsubstituted *p-tert*-butylcalix[6]arene. The lack of any significant difference in activation barrier between 1,3- and 1,4-(thio)phosphorylated derivatives is remarkable. Upon further substitution, the activation free energy gradually decreases and the hexaphosphate **6** has an activation Gibbs free energy for macrocyclic ring interconversion of 59 kJ·mol^{-1}, which is on the same order of magnitude as that for unsubstituted *p-tert*-butylcalix[6]arene[27b] (56 kJ·mol^{-1}). The $\Delta G_m^{\ddagger}$ values for thiophosphates are consequently larger than those for analogous phosphates, which may be attributed to the larger bulkiness of the thiophosphate groups.

The observed tendency of a sharp increase of activation Gibbs free energy upon monosubstitution and gradual decrease of $\Delta G_m^{\ddagger}$ contradicts that upon monosubstitution; the *cyclic* hydrogen bond array of *p-tert*-butylcalix[6]arene is interrupted, which should lead to a decrease of the average strength of the remaining hydrogen bonds and thus to an increase in flexibility. Further substitution should reduce the interconversion barrier even more. This intuitive approach only considers the strength of hydrogen bonds, but not the trajectory of the interconversion process. Depending on the interconversion mechanism, the *O*-substituent or a *p-tert*-butyl group is forced to pass the annulus

of the calix[6]arene skeleton. This action simultaneously disturbs or breaks multiple hydrogen bonds of the well-ordered hydrogen bond array. In the transition state for macrocyclic ring interconversion of *p-tert*-butylcalix[6]arene fewer hydrogen bonds are broken, and as a net effect the activation Gibbs free energy increases. Upon monosubstitution of (*p-tert*-butyl)calix-[4]arene, a similar increase of activation Gibbs free energy for macrocyclic ring interconversion was observed. Groenen *et al*. explained this phenomenon by postulating a concerted macrocyclic ring interconversion pathway.[27c] Calculations, however, showed this hypothesis to be unlikely, and a "broken chain" model has been developed.[44] Yet, similar calculations reveal that *p-tert*-butylcalix[6]arene interconverts most probably via a concerted pathway, in which the hydrogen bond array is preserved in the transition state.[45] In this case, monosubstitution prevents the calix[6]arene from interconverting via a concerted pathway, and concomitantly the energy barrier is raised. Introduction of more substituents of the same type reduces the number of hydrogen bonds at the lower rim, which can be disturbed in the transition state of the interconversion process, while the energy term for steric hindrance remains the same. This will result in a drop of the activation Gibbs free energy. Variation of the substitution pattern does not change the activation barrier to any extent, which is illustrated by the 1,4- and 1,3-diphosphorylated derivatives. This observation points to a similarity in both the strength of the hydrogen bond arrays and transition-state. By the passage of a substituent through the annulus, independent of the substitution pattern, *all* hydrogen bonds will be disturbed.

Hydrogen Bond Array Reversal. As expected, the activation free energy for hydrogen bond reversal is dependent on the number of hydrogen bonds in the array. The value of $\Delta G_h^{\ddagger}$ = 45 kJ·mol^{-1} for mono(thio)phosphates **2** and **7** is on the order of magnitude for that of pinched conformer interconversion (*vide infra*). In this hydrogen bond array five hydrogen bonds are involved, which means an average energy of 9 kJ·mol^{-1} (2 kcal·mol^{-1}) per hydrogen bond as a lower limit. This is a value of an intermediately strong hydrogen bond, which is frequently found in the literature.[35] The lower limit for the average

(44) Fischer, S.; Grootenhuis, P. D. J.; Groenen, L. C.; van Hoorn, W. P.; van Veggel, F. C. J. M.; Reinhoudt, D. N.; Karplus, M. *J. Am. Chem. Soc.* **1995**, *117*, 1611.

(45) Preliminary results from W. P. van Hoorn, which will be published elsewhere; for more information on the TRAVEL module see ref 44.

hydrogen bond strength for 1,4-di(thio)phosphates **4** and **9** is 7.8 kJ·mol^{-1}, and is comparable to that of mono(thio)phosphates **2** and **7**. Hydrogen bond arrays have also been observed in cyclodextrins in the solid state.[26] However, the dynamics of the hydrogen bond array reversal is much faster than observed for the calix[6]arenes.

Pinched Conformer Interconversion. Depending on the type of compound, the activation barriers for pinched conformer interconversion vary between 44 and 55 kJ·mol^{-1} (Table 3). The increase of 10 kJ·mol^{-1} of the barrier for pinched conformer interconversion of 1,4-diphosphate **4** compared to 1,3-diphosphate **3** can only be partly explained by the difference in Gibbs free energy between the major and minor pinched conformers of ca. 4.3 kJ·mol^{-1} (Table 3),[46] and points to additional strain factors in the transition state structure.

Finally, in view of these results, the NMR results reported by Pons *et al.*,[29] which were described in terms of pairwise tilting of aromatic rings of an "open" cone conformation, can alternatively and more elegantly be explained by a concerted pinched conformer and macrocyclic ring interconversion process of a pinched cone conformation.[47] Moreover, the concerted pathway offers a good explanation for the nearly equal activation Gibbs free energies of 12.8 and 12.2 kcal·mol^{-1} they calculated for macrocyclic ring interconversion and "pseudorotation", which are according to us both the activation barrier for the same process.

Conclusions

The dynamics in calix[6]arenes is governed by at least three dynamic processes, e.g., macrocyclic ring interconversion, hydrogen bond array reversal, and pinched conformer interconversion, which can be ranked according their activation barriers as follows: hydrogen bond array reversal < pinched conformer interconversion < macrocyclic ring interconversion.

In solution, hydrogen bond formation forces the calix[6]arene skeleton to be pinched in order to optimize the hydrogen bond geometry, and these conformers may be involved in pinched conformer interconversion. The existence and structure of pinched conformers in solution was demonstrated by their unique exchange connectivity patterns. The hydrogen bond arrays are involved in hydrogen bond array reversal. By macrocyclic ring interconversion the substituents can flip through the annulus according to known mechanisms.[25] The barrier for macrocyclic ring interconversion compared to that of unsubstituted *p-tert*-butylcalix[6]arene is increased most upon monosubstitution with a bulky substituent and gradually decreases, when the degree of substitution is increased. The barrier is hardly influenced by the substitution pattern. In unsubstituted calix[6]arenes, macrocyclic ring and pinched conformer interconversion are coupled in a single process. Other interconversion processes, which can be visualized as the tilting of aromatic rings, like the so-called "pseudorotation" proposed by Pons *et al.*[29] and "pinched cone interconversion" in calix[4]arenes,[23] might also occur more generally in all substituted calix[6]arenes. In our studies these processes have not been observed, and we think that their activation barriers are much lower than the ones listed in Table 3, which makes these processes much faster on the chemical shift time scale at room temperature than the other dynamic processes.

Finally, we feel that the dynamic processes observed in calix-[6]arenes will also occur in all higher calixarenes such as calix-[8]arenes and can be investigated with the same methodology as described in this paper.

Experimental Section

NMR Measurements. NMR measurements were performed at either 250 or 400 MHz, on Bruker AC250 and Varian Unity 400WB spectrometers, respectively. Me$_4$Si was used as the internal standard for ^{1}H and ^{13}C NMR spectroscopy and 80% H$_3$PO$_4$ for ^{31}P NMR spectroscopy, unless stated otherwise. NOESY,[48,49] ROESY,[50] and TOCSY (MLEV17)[51] were performed using standard Varian pulse programs. Relaxation times in the rotating frame ($T_{1\rho}$) were measured by the $(\pi/2)_x$−(spin lock)$_y$ sequence.[37] All TOCSY (MLEV17) experiments were performed with mixing times of 30 ms. The mixing times of the NOESY experiments ranged from 100 to 700 ms. The mixing time of the ROESY experiments consisted of a spin lock pulse of 2 kHz field strength with a duration of 300 ms. All 2D experiments performed on the Unity 400WB were collected, using 2D hypercomplex data.[52] Data were Fourier transformed in the phase-sensitive mode after weighting with shifted square sine bells of shifted Gaussian functions. NMR data were processed either by the standard Varian VnmrS/VnmrX software packages installed on the Unity 400WB spectrometer host computer (SUN Sparc 10) or by the NMRi package installed on a SUN4 computer. Thermodynamic parameters ($\Delta G°$) were calculated from equilibrium constants, which could be derived from signal integrals in 1D ^{31}P NMR spectra recorded at 400 MHz. $\Delta G^{\ddagger}$ values were calculated from interconversion rate constants, which were determined by integration of exchange peaks in EXSY/NOESY experiments.

Synthesis. Melting points are uncorrected. If not mentioned explicitly, ^{1}H and ^{31}P NMR spectra were recorded on a Varian 400 MHz instrument and ^{13}C NMR spectra on a Bruker 250 MHz instrument in CDCl$_3$ with TMS as an internal standard. Preparative column chromatography separations were performed on Merck silica gel 60 (250−400 mesh), while precoated silica gel plates (Merck, 60 F$_{254}$) were used for analytical TLC. FAB mass spectra were performed on a Finnigan MAT 90 spectrometer, with *m*-nitrobenzyl alcohol as a matrix. All solvents were purified by standard procedures. Petroleum ether refers to the fraction with bp 40−60 °C. All other chemicals were analytically pure, and were used without further purification. *p-tert*-Butylcalix[6]arene (**1**) was prepared as described in the literature.[53] All reactions were carried out under a nitrogen atmosphere.

37-[(Diethoxyphosphoryl)oxy]-5,11,17,23,29,35-hexakis(1,1-dimethylethyl)calix[6]arene-38,39,40,41,42-pentol (2). To a solution of *p-tert*-butylcalix[6]arene (**1**) (3.0 g, 3.09 mmol) in CHCl$_3$ (300 mL) were added Et$_3$N (1.28 mL, 9.3 mmol) and diethoxyphosphoryl chloride (0.89 mL, 6.17 mmol). The mixture was refluxed for 6 h. The solution was washed with 1 N HCl (2 × 100 mL), water (100 mL), and brine (50 mL) and dried over MgSO$_4$. The crude residue was purified by column chromatography (silica gel, EtOAc/hexane, 15:85): yield 1.37 g (37%); mp 174−176 °C (MeOH); ^{1}H NMR δ 9.4−9.0 (br m, 3 H, ArOH), 8.4−8.2 (br s, 2 H, ArOH), 7.15−7.1 (m, 6 H, ArH), 7.1−7.05 (m, 4 H, ArH), 6.78 (s, 2 H, ArH), 4.70 and 3.57 (AX, *J* = 14.6 Hz, 2 H, ArCH$_2$Ar), 3.87 and 3.67 (AX, *J* = 13.9 Hz, 2 H, ArCH$_2$-Ar), 3.87 and 3.54 (AX, *J* = 15.5 Hz, 2 H, ArCH$_2$Ar), 4.50−4.35 (m, 4 H, OCH$_2$), 1.46 (dt, J_{HH} = 7.0 Hz, J_{HP} = 0.95 Hz, 6 H, CH$_3$), 1.30, 1.28 [s, 18 H, C(CH$_3$)$_3$], 1.22, 0.94 [s, 9 H, C(CH$_3$)$_3$]; ^{13}C NMR δ 149.0, 148.0, 147.9, 146.9, 144.2, 143.6, 143.3, 131.5, 127.3, 127.2, 126.7 (s, ArC), 127.1, 126.2, 125.8, 125.7, 125.0 (d, ArC), 34.1, 34.0, 33.9 [s, *C*(CH$_3$)$_3$], 32.8, 32.3 (t, ArCH$_2$Ar), 31.6, 31.5, 31.4, 31.1 [q, C(*C*H$_3$)$_3$], 16.2 (q, CH$_3$); ^{31}P NMR δ −4.67; MS (FAB) *m/e* 1109.9 [(M + H)$^+$, calcd 1109.7]. Anal. Calcd for C$_{70}$H$_{93}$O$_9$P·0.17 H$_2$O: C, 75.57; H, 8.46. Found: C, 75.19; H, 8.46. Karl Fischer: H$_2$O, 0.28. C$_{70}$H$_{93}$O$_9$P·0.17H$_2$O requires H$_2$O, 0.28%.

37,39-Bis[(diethoxyphosphoryl)oxy]-5,11,17,23,29,35-hexakis(1,1-dimethylethyl)calix[6]arene-38,40,41,42-tetrol (3) was prepared in a way similar to that of monophosphate **2** starting from *p-tert*-butylcalix-[6]arene (**1**) (4.0 g, 4.1 mmol), Et$_3$N (2.28 mL, 16.5 mmol), and

(46) (a) Hammond, G. S. *J. Am. Chem. Soc.* **1953**, *77*, 334; (b) Farcasiu, D. *J. Chem. Educ.* **1975**, *52*, 76.

(47) The calculated activation Gibbs free energy with the program TRAVEL[44] was 13.0 kcal·mol^{-1}, which closely matches the reported value of 12.8 kcal·mol^{-1}.

(48) Neuhaus, D.; Williamson, M. P. *The Nuclear Overhauser Effect in Structural and Conformational Analysis*; VCH Publishers: Cambridge, U.K., 1989.

(49) Jeener, J.; Meier, B. H.; Bachmann, P.; Ernst, R. R. *J. Chem. Phys.* **1979**, *71*, 4546.

(50) Bothner-By, A. A.; Stephens, R. L.; Lee, L.; Warren, C. D.; Jeanloz, R. W. *J. Am. Chem. Soc.* **1984**, *106*, 811.

(51) Bax, A.; Davis, D. *J. Magn. Reson.* **1985**, *65*, 355.

(52) States, D. J.; Haberkorn, R. A.; Ruben, D. J. *J. Org. Reson.* **1982**, *48*, 286.

(53) Gutsche, C. D.; Dhawan, B.; Leonis, M.; Stewart, D. *Organic Syntheses*; Wiley and Sons: New York, 1993; Collect. Vol. VIII, 77−79.

Table 5. Experimental Data for the X-ray Diffraction Studies on Mono(thiophosphate) **7**

crystal morphology	parallelepipedum	V (Å^3)	3556(1)
formula	C$_{70}$H$_{93}$O$_8$PS·CH$_3$CN·4H$_2$O		
		Z	2
FW	1238.67	d_{calcd} (g cm^{-3})	1.16
crystal system	triclinic	μ (cm^{-1})	10.52
space group	$P\bar{1}$	reflections measured	$\pm h, \pm k, l$
T (K)	173(2)	no. of unique total data	4277
cell parameters		no. of unique obsd data	3831 [$F_0^2 > 3\sigma(F_0^2)$]
a (Å)	14.713(3)	no. of variables	795
b (Å)	16.979(4)	R	0.056
c (Å)	17.023(4)	R_w	0.058
α (deg)	82.23(2)	$(\Delta/\sigma)_{max}$	0.2
β (deg)	64.83(2)		
γ (deg)	67.61(2)		

diethoxyphosphoryl chloride (2.38 mL, 16.5 mmol) in CHCl$_3$ (400 mL). The crude solid after workup was separated by column chromatography (silica gel, EtOAc/hexane, 2:8). Diphosphate **3** was isolated as the second fraction: yield 1.57 g (31%); mp 196−198 °C (MeOH); ^{1}H NMR δ 8.48 (s, 1 H, ArOH), 7.85 (s, 2 H, ArOH), 7.23, 7.15 (s, 2 H, ArH), 7.12, 7.07 (d, J = 2.3 Hz, 2 H, ArH), 6.71, 6.42 (br s, 2 H, ArH), 4.68 and 3.54 (AX, J = 15.4 Hz, 2 H, ArCH$_2$Ar), 4.52 and 3.70 (AX, J = 16.8 Hz, 2 H, ArCH$_2$Ar), 4.4−4.2 (m, 8 H, OCH$_2$), 3.81 and 3.64 (AX, J = 13.8 Hz, 2 H, ArCH$_2$Ar), 1.37, 1.32 [s, 9 H, C(CH$_3$)$_3$], 1.26, 0.86 [s, 18 H, C(CH$_3$)$_3$], 1.4−1.3 (m, 12 H, CH$_3$); ^{13}C NMR δ 150.0, 149.1, 148.8, 147.9, 147.4, 143.5, 142.9, 142.8, 142.5, 131.8, 131.7, 131.6, 127.5, 126.8, 126.5 (s, ArC), 126.0, 125.4, 124.7, 123.7 (d, ArC), 65.4 (t, OCH$_2$), 34.0, 33.9 [s, C(CH$_3$)$_3$], 32.4, 31.7, 31.6 (t, ArCH$_2$Ar), 31.5, 31.0 [q, C(CH$_3$)$_3$], 16.1 (q, CH$_3$); ^{31}P NMR δ −4.1; MS (FAB) m/e 1245.7 [(M + H)$^+$, calcd 1245.7]. Anal. Calcd for C$_{74}$H$_{102}$O$_{12}$P$_2$·0.5 H$_2$O: C, 70.85; H, 8.28. Found: C, 70.50; H, 8.07. Karl Fischer: H$_2$O, 0.78. C$_{74}$H$_{102}$O$_{12}$P$_2$·0.50 H$_2$O requires H$_2$O, 0.72%.

37,40-Bis[(diethoxyphosphoryl)oxy]-5,11,17,23,29,35-hexakis(1,1-dimethylethyl)calix[6]arene-38,39,41,42-tetrol (4) was isolated as the first fraction from the chromatographical separation of diphosphate **3**: yield 1.41 g (27%); mp 249−251 °C (MeOH); ^{1}H NMR δ 8.6−8.2 (br s, 4 H, ArOH), 7.23, 7.05 (d, 4 H, J = 2.3 Hz, ArH), 6.7−6.5 (br s, 4 H, ArH), 4.7−4.4 (br s, 4 H, ArCH$_{2,ax}$Ar), 4.4−4.0 (br m, 10 H, ArCH$_{2,ax}$Ar, OCH$_2$), 3.8−3.3 (br m, 6 H, ArCH$_{2,eq}$Ar), 1.29 [s, 36 H, C(CH$_3$)$_3$], 1.04 (t, 12 H, CH$_3$), 0.8−0.6 [s, 12 H, C(CH$_3$)$_3$]; ^{13}C NMR δ 149.5, 147.5, 142.3, 131.4, 131.3, 127.3, 124.7 (s, ArC), 126.0, 124.6 (d, ArC), 65.7 (t, OCH$_2$), 33.9 [s, C(CH$_3$)$_3$], 31.6, 30.8 [q, C(CH$_3$)$_3$], 15.7 (q, CH$_3$); ^{31}P NMR δ −4.39; MS (FAB) m/e 1245.7 [(M + H)$^+$, calcd 1245.7]. Anal. Calcd for C$_{74}$H$_{102}$O$_{12}$P$_2$: C, 71.36; H, 8.25. Found: C, 71.24; H, 8.27.

37,38,40-Tris[(diethoxyphosphoryl)oxy]-5,11,17,23,29,35-hexakis-(1,1-dimethylethyl)calix[6]arene-39,41,42-triol (5) was prepared in a reaction similar to that of monophosphate **2** starting from *p-tert*-butylcalix[6]arene (**1**) (3.0 g, 3.1 mmol), Et$_3$N (12 mL, 86.7 mmol), and diethoxyphosphoryl chloride (2.68 mL, 18.5 mmol) in CHCl$_3$ (300 mL). The crude solid after workup was separated by column chromatography (silica gel, EtOAc/hexane, 3:7). As a first fraction, 1,4-diphosphate **4** was eluted (980 mg, 25%). The second fraction consisted of crude **5**, which was recrystallized from MeOH/water: yield 1.97 g (46%); mp 158−160 °C (MeOH); ^{1}H NMR δ 7.8−6.4 (br m, 15 H, ArH, ArOH), 4.8−3.0 (br m, 24 H, ArCH$_2$Ar, OCH$_2$), 1.5−0.6 (br m, 72 H, C(CH$_3$)$_3$, CH$_3$); ^{31}P NMR δ −4.3, −4.5, −5.7; MS (FAB) m/e 1382.5 [(M + H)$^+$, calcd 1381.7]. Anal. Calcd for C$_{78}$H$_{111}$-O$_{15}$P$_3$·H$_2$O: C, 66.93; H, 8.14. Found: C, 67.29; H, 8.16. Karl Fischer: H$_2$O, 1.2. C$_{78}$H$_{111}$O$_{15}$P$_3$·H$_2$O requires H$_2$O, 1.3%.

37,38,39,40,41,42-Hexakis[(diethoxyphosphoryl)oxy]-5,11,17,23,-29,35-hexakis(1,1-dimethylethyl)calix[6]arene (6). To a solution of *p-tert*-butylcalix[6]arene (**1**) (3.0 g, 3.1 mmol) in CH$_2$Cl$_2$ (120 mL) were added freshly ground NaOH (3.0 g, 75 mmol), diethoxyphosphoryl chloride (4.45 mL, 30.8 mL), and tetrabutylammonium bromide (0.3

g). The suspension was stirred for 24 h at room temperature (rt). The organic layer was then washed with 1 N HCl (2 × 50 mL), water (2 × 25 mL), and brine (1 × 25 mL) and dried over MgSO$_4$. The crude solid was separated by column chromatography (silica gel). Elution was started with EtOAc and then with EtOAc/MeOH, 8:2. The crude hexaphosphate was recrystallized from MeOH/water: yield 2.0 g (36%); mp 275−276 °C (EtOAc/hexane); ^{1}H NMR δ 7.6−6.8 (br m, 12 H, ArH), 5.0−3.4 (br m, 36 H, ArCH$_2$Ar, OCH$_2$), 1.6−0.4 (br m, 90 H, C(CH$_3$)$_3$, CH$_3$); ^{31}P NMR δ −4.8; MS (FAB) m/e 1790.1 [(M + H)$^+$, calcd 1789.8]. Anal. Calcd for C$_{90}$H$_{138}$O$_{24}$P$_6$: C, 60.39; H, 7.77. Found: C, 60.41; H, 7.96.

X-ray Diffraction. The X-ray measurement was performed on an Enraf-Nonius CAD4 single-crystal diffractometer. The structure was solved and refined using the Enraf-Nonius package of crystallographic computer programs.[54] Reflections for mono(thiophosphate) **7** were measured with graphite-monochromated Cu Kα radiation (λ = 1.5418 Å). The most important crystallographic data are collected in Table 5. Reflections were measured in the $\omega/2\theta$ scan mode [scan width (ω) = (1.1 + 0.2 tan θ)°; 2.5° < θ < 40°]. Refinement was carried out by full matrix least squares. Scattering factors were taken from the *International Tables for X-ray Crystallography*.[55] All calculations were performed on a VAX station 3100/M76 of the Laboratory of Chemical Physics at the University of Twente, the Netherlands.

Refinements were started with one calix[4]arene and one acetonitrile molecule in the asymmetric unit. A difference Fourier synthesis calculated after the refinement showed four peaks which were included as (partially occupied) oxygen positions in the refinement. These peaks are assumed to be due to cocrystallizing water molecules. The number of parameters refined is 795 (scale factor, extinction factor, positional parameters, (an)isotropic thermal parameters). All atoms other than hydrogen were refined with anisotropic thermal parameters with the exception of two water oxygens, which were refined isotropically. Hydroxyl hydrogen atoms were found from a difference Fourier synthesis and refined with isotropic thermal parameters. All other hydrogens were put on calculated positions. Hydrogens of the water molecules and the acetonitrile molecule could not be located, owing to the rather high thermal motion or disorder.

Supporting Information Available: Tables of positional and thermal parameters, bond lengths, and bond angles for **7** (11 pages). This material is contained in many libraries on microfiche, immediately follows this article in the microfilm version of the journal, can be ordered from the ACS, and can be downloaded from the Internet; see any current masthead page for ordering information and Internet access instruction.

JA9540942

(54) Structure Determination Package: B. A. Frenz and Associates, Inc., College Station, TX, and Enraf-Nonius, Delft, The Netherlands, 1983.

(55) *International Tables for X-ray Crystallography*; Kynoch Press: Birmingham, England, 1974; Vol. IV; Distr. Kluwer Academic Publishers: Dordrecht, The Netherlands.